JOSEPH F. BIRD and RICHARD A. FARRELL

ELECTROMAGNETIC SCATTERING THEORY

Various theoretical investigations of electromagnetic scattering are reviewed that illustrate the interplay between basic researches and application needs. Topics covered include stochastic variational techniques for vector wave scattering by random systems of general electromagnetic properties, such as rough surfaces or chaff clouds; the development of simple but effective trial functions for variational usage; and the treatment of electromagnetic induction and color vision as vector field scattering problems.

INTRODUCTION

The purpose of this article is to survey selected aspects of the basic research program in electromagnetic scattering theory that is conducted by the Theoretical Problems Group of APL's Milton S. Eisenhower Research Center. In the process, we shall indicate the interrelations between this research program and mission requirements in other departments of APL. In general, the interconnections come about through collaboration with another department in one of two ways. A technical problem may be uncovered whose solution requires the development of fundamental sciences, e.g., the needs for a broadband method of analysis of radar scatter by the sea surface and for investigation of hydromagnetic signals in the ocean. Or a problem may arise whose solution involves scientific techniques developed in other applications, e.g., the analyses of the magnetic suspension in satellite disturbance compensation systems (DISCOS) and of experiments in color vision.

The propagation, scattering, and absorption of electromagnetic and other waves provide potential tools for probing various media, such as the ocean's surface, particulate matter in the ocean, chaff (and other obscurants), aerosols, bubbles, and military targets. These phenomena have been important to the tasks of APL since its inception, for the specification, design, and use of such systems as radar, sonar, altimeters, and radio communication links. Also, from time to time technologic problems in other areas arise at APL or in other Johns Hopkins Divisions, e.g., corneal light scattering, color vision analysis, and electromagnetic induction effects, which in our experience can be attacked fruitfully by vector-field wave scattering techniques.

Surveying a representative sample of such researches entails a rather lengthy article, and its theoretical character involves considerable mathematics. However, the most rigorous section (Eqs. 6 through 22) may be skimmed or skipped without impaired understanding of subsequent sections.

OVERVIEW

Many macroscopic phenomena are manifestations of electromagnetic field interactions with inhomogeneous media and discrete bodies, all possessing a variety of material properties. Such "scattering," in a general sense, includes wave reflection, refraction, diffraction, or absorption phenomena, as well as more slowly varying inductive interactions. In general, the electromagnetic field varying in space and time can be Fourier analyzed into elemental waves over a spectrum of frequencies. At frequencies below those at which quantum effects dominate, the classical electromagnetic field theory usually is adequate to describe scattering phenomena. This classical regime can extend over 15 decades of frequency in hertz—from the optical through microwave and radio bands down through quasistationary induction to the zero-frequency static limit.

The Group has pursued a long-standing basic research program in the theory of electromagnetic wave scattering. Since the electromagnetic field is a vector, vector-wave theory is used, but special cases of scalar waves also relevant to acoustics have been considered. Naturally, much effort has focused on the electromagnetic wave scattering because of its greater difficulty and the importance of optical, radar, and induction technology to APL missions. Classical methods of vector field theory are used, with emphasis on the powerful variational technique.[1]

Classical field theories are typically expressed in terms of partial differential equations with associated boundary conditions. Alternatively, the method of Green's functions can be employed to obtain an integral representation for the field. In the latter, a scattered field is expressed in terms of integrals that depend on the unknown field on and within the scatterers. An efficient method of solution is to use physical intuition to obtain trial approximations for the fields at the scatterers and then calculate the scattered field by evaluating the integrals. Of course, any errors in the chosen trial fields will generally result in errors of the same relative order in the calculated scattered field.

The Schwinger variational principle[2] is an extremely important contribution in that it recasts the integral representation into an invariant form, that is, an expression in which first-order errors in the trial fields lead only to second-order errors in the calculated scattered field. Thus, this variational principle enables one to improve existing approximations. It also facilitates

the design of new trial approximations that are effective and yet simple. However, the absence of first-order errors in the variational formulation is obtained at the cost of replacing a single integral by a quotient that involves the product of two such integrals divided by a third (more complicated) integral. Thus, although the method has been applied to a variety of problems,[1-8] only limited application[9,10] was made relevant to stochastic scattering problems, i.e., random ensembles of scatterers such as the ocean's surface or rain clouds.[11] The apparent need to evaluate statistical averages of the quotient of integrals would certainly discourage such application.

The development of variational techniques as a calculational tool for stochastic scattering problems has been a central goal of the Group's program. A breakthrough was achieved when we obtained an alternative invariant stochastic formulation.[12] Specifically, when the integrals appearing in the above-mentioned quotient are first averaged and then the quotient is taken, one has an invariant expression for the averaged scattered field. This form is inherently simpler to evaluate than the average of the quotient, yet is variationally equivalent to it. As will be discussed, the research effort so far has culminated in a general stochastic variational principle (SVP) for electromagnetic scattering by arbitrary random distributions of scatterers with any linear electric and magnetic properties.

These wave-scattering studies, initiated in support of the submarine security program by R. W. Hart, then chairman of the Research Center, led first to a scalar form of the SVP.[12] The motive for this research was to facilitate analysis of radar returns from sea-surface "scars" left by submarines. Because the scars contained roughness scales of the order of radar wavelength (as well as larger and smaller scales), it was desirable to improve on standard "two-scale" theory.[13] That analysis uses a long-wavelength (perturbation) approximation for small vertical roughnesses and a short wavelength (Kirchhoff) approximation for large horizontal scales (Fig. 1a). This leaves untreated the roughness features comparable to wavelength in both height and breadth. Thus there was a need to develop a fundamental theory that remained valid through the transition region. This central omission has received prominent attention only very recently,[14-17] though still with limitations (e.g., neglect of multiple scattering). In contrast, early tests of the scalar SVP showed that it can account largely for multiple scattering well into the transition regime.[18-21]

Subsequent work has been directed toward developing and testing the SVP as a calculational tool. This has been accomplished largely in collaboration with the Fleet Systems Department.[19-29] It formed the basis for a Ph.D. thesis and a post-doctoral research project of staff members now in that department. The work has produced a dyadic SVP that is applicable to vector wave scatterers of arbitrary inhomogeneous and anisotropic permittivity, conductivity, and permeability, possessing arbitrary random characteristics. The dyadic (i.e., vectorvector, or second-rank three-dimensional tensor) formulation is desirable because it allows one to account for the anisotropy of the material properties through which an electromagnetic field vector in one direction can produce polarization, magnetization, or current vectors in other directions. The dyadic formalism also facilitates the Green's function solution of the governing vector equations. Test application has shown that the SVP can account for polarization, interference, and multiple-scattering effects—even with simple trial functions that do not yield these effects in standard noninvariant calculations.[25,26] The tests used trial approximations valid at long wavelengths and showed that the variational technique extended their range of validity to include roughness scales up to the order of the wavelength.

Recent effort has focused on trial-function selection and design to achieve accurate but tractable broadband scattering calculation.[27-30] The initial work again concerned long wavelengths.[27] Then, as a next step toward variational improvement of "two-scale" theory, variational treatment of a short wavelength (Kirchhoff)

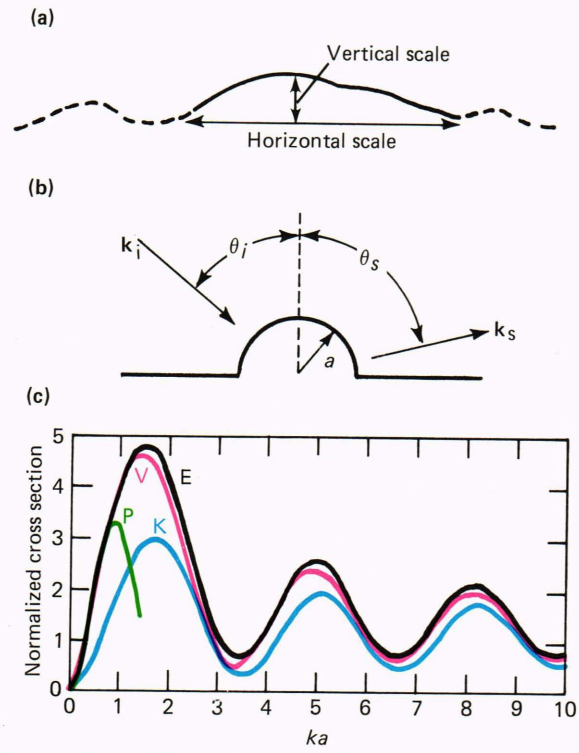

Figure 1—(a) Schematic of rough-surface element. (b) Rayleigh model: Circular cylindrical boss (radius *a*) on a perfectly conducting plane with a plane-wave (vector $\mathbf{k}_i$) incident at the angle θ_i and scattering into directions θ_s (defining a scattered wave vector $\mathbf{k}_s$). (c) Relative scattering cross sections as functions of the size/wavelength parameter (*ka*) for the Rayleigh model above for $\theta_i = \theta_s = 0$ and horizontal polarization. Curves denote results for perturbation (P) and Kirchhoff (K) approximations, for the variational improvement (V) of the latter, and for the exact solution (E). Note that whereas P and K depart from E at $ka \gtrsim 1$ and $ka \lesssim 3$, respectively, the variational curve V follows E from large *ka* nicely through the gap ($ka \sim 3$ to 1) down to $ka = 0$. Even more accurate broadband results have been achieved with novel, yet simple trial functions, as illustrated in Fig. 8.

trial field was carried out for a test surface. As illustrated in Fig. 1a, a rough surface is described by vertical deviation as a function of horizontal dimensions, which includes height, slopes, curvatures, and higher variations. A tractable test model for analysis is Rayleigh's classic surface-scattering model, a circular hemicylindrical boss on a perfectly conducting plane, as depicted in Fig. 1b. For that model, all the vertical-horizontal variation scales are represented just by the boss radius, a. Thus a unique size/wavelength ratio parameterizes the model, viz., ka, where $k \equiv 2\pi/\lambda$ is the wavenumber of the incident radiation of wavelength λ. More importantly, the model has a tractable exact solution to which we may compare different approximate solutions. This is important because it is the only ironclad way to assess the accuracy of approximation methods. Such a comparison is displayed in Fig. 1c for the initial case we treated—backscatter of normally incident, horizontally polarized waves. One sees from this graph (with the exact solution, curve E, as benchmark) that the long-wave perturbation result (curve P) is satisfactory for small ka but fails badly for $ka \gtrsim 1$, while the short-wave Kirchhoff result (curve K) may be acceptable for large ka but fails badly at $ka \lesssim 2$. In contrast, the variational result (curve V) shows good agreement at *all* wavelengths, i.e., not only from high frequencies into the transition region, as hoped, but all the way through to the low-frequency (Rayleigh) limit.[28] (Other examples of this all-frequency variational improvement at different angles and polarization are shown in Figs. 6 and 7.)

Although detailed analysis for this model over all polarizations and angles showed that the all-frequency improvement was not fully satisfactory,[30] these studies encouraged subsequent attempts to design new trial functions for accurate broadband scattering calculations.[28,29] For perfect conductors, we modified the long-wavelength trial fields so that they became capable of satisfying the boundary conditions. At least for simple test models, this approach has yielded extremely accurate all-frequency variational results.[29] (An example is displayed in Fig. 8.) Presently, in collaboration with the Space Department, similar methods are being tried on models for ocean surface radar scatter. Future studies will be directed at surfaces with arbitrary electromagnetic properties, where the fields penetrate the surface.

Most of this article will be devoted to elaborating on the SVP theory and its applications. However, we also present brief descriptions of some of the other electromagnetic scattering research that the Group has done in collaboration with colleagues from other APL departments or from other divisions of Johns Hopkins. In long-standing biomedical research collaboration with the Johns Hopkins Medical Institutions, a major eye corneal structure program has investigated both visible light scattering and infrared absorption in the cornea. An intricate interplay between experiment and theory led to the development of light scattering as a tool to probe the ultrastructure of the cornea and yielded an explanation of infrared damage to corneal cells. These studies of electromagnetic interactions with biological tissue were surveyed recently in the *Johns Hopkins APL Technical Digest,*[31] and extensions of the infrared studies are described in the article by McCally et al. elsewhere in this issue. In another biomedical effort with the Johns Hopkins Medical Institutions, early APL vision research eventuated in a general vector field theory of vision, considered as the "scattering" process first defined and investigated by Maxwell: electromagnetic field absorptions at the retina transmuting into a brightness-color spatiotemporal sensation field.[32,33] Concomitant electrophysiological studies with APL's Biomedical Programs Office suggested a novel electroretinographic analysis technique.[34]

Finally, various problems in electromagnetic induction that have concerned different departments of APL have been attacked via vector-field methods with considerable success. Thus, analyses of hydromagnetism induced by ocean motion across the geomagnetic field, initiated for the SSBN security program, yielded many useful numerical estimates, proved a new eddy theorem, identified the phenomenon of sonomagnetic pseudowaves (hydromagnetic fields propagated via acoustic radiation), and determined their scattering by the air-sea surface.[35-38] For the Space Department, levitational force-torque in the magnetic suspension of the disturbance compensation system (DISCOS), now deployed in NOVA satellites, was analyzed to aid in malfunction diagnosis and design optimization for DISCOS. The power of vector field analysis is exemplified by the fact that the analysis produced both significant practical design simplification and new contributions to magnetic levitation theory.[39-41]

STOCHASTIC VARIATIONAL PRINCIPLES

General features of variational principles that make them invaluable as calculation tools are reviewed briefly in this section. The generic form of the Schwinger-type variational principle is discussed, without making explicit the integrals that compose it; these are given in the next section. After pointing out the difficulty of applying the Schwinger form to stochastic scatterers, the APL-developed stochastic version of this principle is presented and discussed.

Many physical problems can be expressed in terms of a set of field functions, Ψ, that obey certain field equations. Often, primary interest is not so much in accurate calculations of Ψ, but in some related quantity, F (e.g., scattering cross section), that can be written as a functional of the field functions, $F(\Psi)$, in various ways. A particular functional is said to be a variational principle if it is invariant for Ψ approaching the exact solution Ψ^E, i.e., if $\delta F(\Psi) \equiv F(\Psi^E + \delta\Psi) - F(\Psi^E) = 0$ to first-order in small variations, $\delta\Psi$. When F is formulated such that the invariance (Euler) equations reproduce the original field equations, $\delta F = 0$ represents a compact statement equivalent to the original problem. Further, since the form of F is chosen such that $F(\Psi^E)$ represents a desired result in the problem, the variational principle offers a power-

ful method of approximately calculating that result from reasonably accurate approximate values of the field Ψ. The variational method may be used either to improve an existing approximation or to fashion efficient new trial approximations. In either case, by virtue of the variational invariance, small errors in the trial functions for the field Ψ lead to much (quadratically) smaller errors in the calculated quantity, F. Indeed, judicious selection of trial fields Ψ such that they can mimic exact behavior where important, viz., in F, no matter how poorly they may behave elsewhere, will be seen to yield efficient and accurate approximations.

An attractive form of variational principle is the Schwinger type, which is a ratio of functionals that is independent of the overall amplitude of the trial function. For example, consider scalar wave problems consisting of a plane wave of amplitude A, frequency ω, and wave vector $\mathbf{k}_i$, viz., $A \exp[i(\mathbf{k}_i \cdot \mathbf{r} - \omega t)]$, interacting with a scatterer to produce a superposition of harmonic waves, say $\psi(\mathbf{r}) \exp(-i\omega t)$. The field distribution near the scatterer may be quite intricate, but interest often centers on the far field ($r \gg$ scatterer size), where the scattered waves reduce to a spherical wave whose amplitude varies with scattering direction denoted by unit vector $\hat{k}_s$. Thus, the field $\psi(\mathbf{r})$ becomes asymptotically the sum of incident plane and scattered spherical fields,

$$\psi(\mathbf{r}) \approx A \exp(i\mathbf{k}_i \cdot \mathbf{r}) + T(\mathbf{k}_s, \mathbf{k}_i) \cdot A \exp(ikr)/r \, , \quad (1)$$

where k denotes wave vector magnitude $|\mathbf{k}_i|$, and $\mathbf{k}_s \equiv k \hat{k}_s$. The key ingredient in Eq. 1 is T, the relative amplitude of the scattered wave, whose determination represents a complete solution for the far-field scattering. For example, the differential cross section is given by $|T|^2$.

The Schwinger variational principle for scatter amplitude T is obtained by considering the adjoint field distribution, $\tilde{\psi}(\mathbf{r})$, which describes the reciprocal problem of a plane wave with wave vector $-\mathbf{k}_s$ scattering into the direction $-\mathbf{k}_i$ (i.e., transforming $\mathbf{k}_s \leftrightarrow -\mathbf{k}_i$ in the original problem). As will be illustrated by the general vector derivation given in the next section, one way to derive Schwinger's expression is to use $\tilde{\psi}$ to eliminate the incident amplitude A and thereby obtain the homogeneous, symmetric variational principle for the scatter amplitude,

$$T^V(\psi, \tilde{\psi}) = N_1(\psi) N_2(\tilde{\psi}) / 4\pi D(\psi, \tilde{\psi}) \, . \quad (2)$$

This functional T^V of the field functions $\psi, \tilde{\psi}$ possesses the valuable invariance properties discussed above (identify Ψ as $\psi, \tilde{\psi}$ and F as T^V), provided the functionals N_1, N_2, and D in Eq. 2 are appropriately defined. This will be seen in detail for the general vector case in the next section, where N_1, N_2, and D are exhibited to be integrals over the field distribution *at* the scatterer. The integral $N_1(\psi)$ is proportional to a known *non*invariant expression for T, while $N_2(\tilde{\psi})$ is the analogous expression in the adjoint problem. The denominator $D(\psi, \tilde{\psi})$ is a double integral whose integrand contains the fields and the Green's function $[G(\mathbf{r}, \mathbf{r}')]$ appropriate to the scattering problem.

The form of Eq. 2 shows that variational invariance is obtained at the extra cost of evaluating the integrals N_2 and D, once the noninvariant solution N_1 is known. Because $\tilde{\psi}$ is the solution to the adjoint problem in which $\mathbf{k}_s \leftrightarrow -\mathbf{k}_i$, it is convenient to use trial fields for the reciprocal problem, $\tilde{\psi}^t$, that are obtained from the trial field for the original problem, ψ^t, also by the transformation $\mathbf{k}_s \leftrightarrow -\mathbf{k}_i$. In that case, not only is it true that $N_2(\tilde{\psi}) = N_1(\psi)$, but also that $N_2(\tilde{\psi}^t) = N_1(\psi^t)$, so that the only additional cost of invariance is to evaluate D. Several specific examples of invariant formulations of scalar problems are given in Ref. 1 (pp. 1128-1134), and a few are presented in the next section.

Vector wave (electromagnetic) scattering has a variational principle of the same generic form as Eq. 2, with ψ now the electromagnetic field represented by $\mathbf{E}$:

$$T^V(\mathbf{E}, \tilde{\mathbf{E}}) = N_1(\mathbf{E}) N_2(\tilde{\mathbf{E}}) / 4\pi D(\mathbf{E}, \tilde{\mathbf{E}}) \, , \quad (3)$$

where T is any component of the vector scatter amplitude. The adjoint field $\tilde{\mathbf{E}}$ and the integrals N_1, N_2, and D are identified in the next section. Here we only note that the integrals are more complex than in the scalar case because their integrands involve dyadic operations on the vector $\mathbf{E}, \tilde{\mathbf{E}}$ field. Like the scalar wave principle (Eq. 2), the vector wave principle (Eq. 3) was initially derived for deterministic scatterers in which the scatterers have no element of randomness. Of course, there are important applications (such as sea surface or chaff cloud scattering) in which the scattering system is necessarily treated as a random ensemble of scatterers (of sea waves or chaff particles), i.e., as a stochastic scatterer.

Stochastic scattering presented a seemingly insuperable difficulty for the Schwinger-type variational principles (Eqs. 2 and 3). When a scatterer is characterized by randomness in its geometrical or material properties, the quantity of interest is a statistical moment of T or of the differential cross section, $|T|^2$. Even the first moment of Eqs. 2 and 3 involves averaging a quotient of complicated integrals,

$$\langle T^V \rangle = \langle N_1 N_2 / 4\pi D \rangle \, , \quad (4)$$

which is generally intractable and deterred application. But this impasse is broken by the work at APL reported in Ref. 12, which demonstrates that, for *arbitrary* scatterer statistics, the integrals N_1, N_2, and D in Eq. 2 can be individually averaged and then recombined to form an invariant ratio for the averaged amplitude. Subsequent work at APL has extended this result to the vector case, Eq. 3, and to all higher moments.[22,23,29] Thus, in lieu of Eq. 4 a *general stochastic variational principle* for mean amplitude is

$$\langle T \rangle^V = \langle N_1 \rangle \langle N_2 \rangle / 4\pi \langle D \rangle \, , \quad (5)$$

in the sense that $\langle T \rangle^V$ is exact when exact fields are

used to evaluate it and that $\delta\langle T\rangle^V = 0$ to first order (cf. above). Note that this is not a claim that Eq. 5 is equal to Eq. 4 (except for exact fields), but simply variationally equivalent to it in that first-order terms vanish; the nonvanishing higher order terms in Eq. 5 differ from those in Eq. 4. Analogous variational expressions hold for higher statistical moments, e.g., $\langle|T|^{2n}\rangle^V = \langle|N_1|^{2n}\rangle\langle|N_2|^{2n}\rangle/(4\pi)^{2n}\langle|D|^{2n}\rangle$.

These SVPs rest on the *sole* assumption that the incident amplitude, A, is not stochastic, whence their proof follows by manipulation[12,22] of the general relations $T = N_1/4\pi A$ and $D = N_2 \cdot A$, which obtain in the derivation of deterministic Schwinger principles (e.g., Eqs. 12 and 14 below). The SVP, Eq. 5, is inherently more tractable than Eq. 4, since evaluating a quotient of averages is less difficult than evaluating averages of quotients. A special case of Eq. 5 was given passing notice (but with neither proof nor subsequent generalization or application) in an early rough-surface scattering theory.[9] Sample results of our SVP applications will be given shortly, but first we will outline the derivation and some important aspects of the general vector variational principle.

VARIATIONAL EXPRESSIONS FOR GENERAL SCATTERING PROBLEMS

The application of variational principles to scattering problems requires explicit expressions for the integrals N_1, N_2, and D. This section presents these expressions for several cases and reviews the derivation of the vector variational principle. These mathematical considerations are the foundation for applications and for the analyses of test cases described in the next section. The comparisons there between the exact and variational results for these test cases provide a measure of the potential utility of variational methods. That section and all subsequent ones have been written in such manner that they can be read without an appreciation for the mathematical foundations presented in this section.

Scalar wave scattering is applicable to acoustics and to electromagnetics with special geometries. As discussed in Ref. 1, scattering from a perfectly conducting cylinder leads to

$$N_1(\psi) = \int dS\, \psi(\mathbf{r}) \times \mathfrak{D}^{\pm}(n) \times \exp(-i\mathbf{k}_s \cdot \mathbf{r});$$

$$D(\psi,\tilde{\psi}) = \int dS \int dS'\, \psi(r)\, \tilde{\psi}(r') \times \mathfrak{D}^{\pm}(n)\, \mathfrak{D}^{\pm}(n') \times G(\mathbf{r},\mathbf{r}'), \tag{6}$$

and reciprocity as indicated earlier yields $N_2(\tilde{\psi}) = N_1(\psi)$. In Eq. 6, S denotes scattering surface, $\mathfrak{D}^{\pm}(n)$ denotes normal derivate $\partial/\partial n$ operating to the right (+) or left (–) for vertical or horizontal polarization, respectively, and $G(\mathbf{r},\mathbf{r}')$ is the Helmholtz Green's function $\exp(ik|\mathbf{r}'-\mathbf{r}|)/4\pi|\mathbf{r}'-\mathbf{r}|$. For the acoustic problem, hard (soft) scatterers correspond to vertical (horizontal) polarization, and scatterer geometry is arbitrary. For another example, in the case of a lossy dielectric body with complex index of refraction, m,

$$N_1(\psi) = \int dV \exp(-i\mathbf{k}_s \cdot \mathbf{r})\, u(\mathbf{r})\, \psi(\mathbf{r}),$$

$$D(\psi,\tilde{\psi}) = \int dV\, u(\mathbf{r})\, \psi(\mathbf{r}) \times \left\{\tilde{\psi}(\mathbf{r}) - \int dV' G(\mathbf{r},\mathbf{r}')\, u(\mathbf{r}')\, \tilde{\psi}(\mathbf{r}')\right\}, \tag{7}$$

where V is the scatterer volume and $u(\mathbf{r}) \equiv k^2(m^2 - 1)$, assuming $m = 1$ (i.e., $u = 0$) outside V, and, again, $N_2(\tilde{\psi}) = N_1(\psi)$. The scalar principle discussed in Ref. 1 is sufficient for the geometries of simple test problems, but practical applications will require the more general vector principle about to be discussed.

Scattering from an object or surface with general electric and magnetic properties (Fig. 2) is described by the vector time-harmonic wave equation for the electric field,

$$\nabla \times \nabla \times \mathbf{E} - k^2\mathbf{E} = \vec{\mathbf{O}} \cdot \mathbf{E}, \tag{8}$$

where k is the wavenumber of an incoming plane wave $\mathbf{E}_i = A\hat{e}_i \exp(i\mathbf{k}_i \cdot \mathbf{r})$ of amplitude A, propagating in the direction $\mathbf{k}_i$ with linear polarization $\hat{e}_i$, and the dyadic operator $\vec{\mathbf{O}}$ characterizes the geometric and material properties of the scatterer. For notational simplification, arguments of functions will be omitted when no confusion can arise. The explicit form of $\vec{\mathbf{O}} \cdot \mathbf{E}$ for general inhomogeneous and anisotropic scatterers with tensor permeability $\vec{\mu}$, permittivity $\vec{\epsilon}$, and conductivity $\vec{\sigma}$, is

$$\vec{\mathbf{O}} \cdot \mathbf{E} = \vec{\mathbf{U}} \cdot \mathbf{E} + \nabla \times \{\vec{\rho} \cdot [\nabla \times \mathbf{E}]\}, \tag{9}$$

where, with $\vec{\mathbf{I}}$ the unit dyadic,

$$\vec{\mathbf{U}} \equiv k^2[\vec{\epsilon} + (4\pi i/\omega)\vec{\sigma} - \vec{\mathbf{I}}], \tag{9a}$$

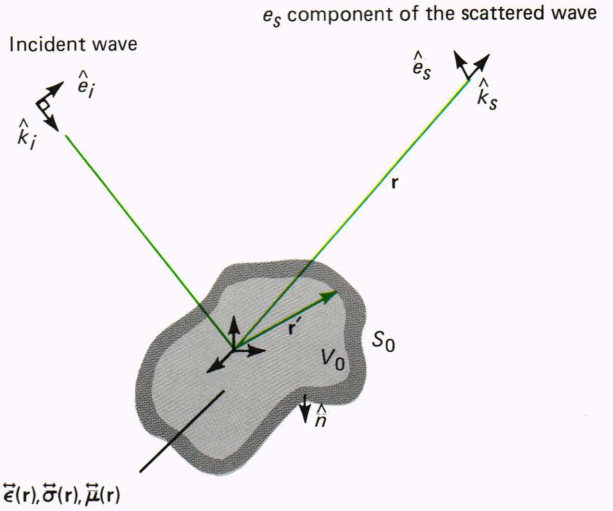

Figure 2—Vector wave scattering from volume V_0, bounded by surface S_0, of material with inhomogeneous anisotropic permittivity, conductivity, and permeability tensors $\vec{\epsilon}(\mathbf{r})$, $\vec{\sigma}(\mathbf{r})$, and $\vec{\mu}(\mathbf{r})$.

$$\overleftrightarrow{\rho} \equiv [\overleftrightarrow{I} - \overleftrightarrow{\mu}^{-1}] \ . \tag{9b}$$

The permittivity and permeability have been normalized by those of the homogeneous background medium in which the scatterers are assumed embedded, and the superscript -1 indicates matrix inversion.

A careful application of Green's theorem yields the integral equation[42,43]

$$\mathbf{E}(\mathbf{r}) = \mathbf{E}_i(\mathbf{r}) + \int_{V_0} dV' \, \overleftrightarrow{G}_0(\mathbf{r},\mathbf{r}') \cdot [\overleftrightarrow{O}(\mathbf{r}') \cdot \mathbf{E}(\mathbf{r}')] \ , \tag{10}$$

where V_0 is the volume of the scatterer and the infinite space Green's dyadic is given by[43]

$$\overleftrightarrow{G}_0(\mathbf{r},\mathbf{r}') = \text{P.V.} \left(\overleftrightarrow{I} + \nabla\nabla/k^2\right) \frac{\exp(ik|\mathbf{r} - \mathbf{r}'|)}{4\pi|\mathbf{r} - \mathbf{r}'|} - \frac{1}{k^2} \overleftrightarrow{L}\delta(\mathbf{r} - \mathbf{r}') \ , \tag{11}$$

where the symbol P.V. implies a principal value when the term in brackets in Eq. 10 is integrated and $\overleftrightarrow{L}$ is the depolarization tensor[44] appropriate to the excluded volume used to define the principal value. The infinite-space Green's dyadic reduces to the usual free space Green's dyadic[42] if the field point $\mathbf{r}$ lies outside the source region V_0, since $\delta(\mathbf{r} - \mathbf{r}') = 0$, and the principal value designation is unnecessary in that event. The form of the infinite-space Green's dyadic can be derived by using the free-space Green's dyadic and Green's vector theorem to derive an integral equation for the field within the source region. The singular nature of $\nabla\nabla(1/|\mathbf{r} - \mathbf{r}'|)$ requires that the point $\mathbf{r} = \mathbf{r}'$ be excluded from the region to which Green's theorem is applied. Removal of an infinitesimal region about $\mathbf{r} = \mathbf{r}'$ yields the principal value integral, and the resultant integral over the surface enclosing this excluded volume yields the $\overleftrightarrow{L}\delta(\mathbf{r} - \mathbf{r}')$ term.[43,45]

The component of the scattering amplitude polarized along a direction $\hat{e}_s$ is obtained from the asymptotic form of Eq. 10 on letting $\mathbf{r} \to \infty$ in Eq. 11, and one finds

$$T \equiv \hat{e}_s \cdot \mathbf{T} = \frac{1}{4\pi A} N_1 \ , \tag{12}$$

$$N_1 \equiv \int_{V_0} dV \, \hat{e}_s \exp(-i\mathbf{k}_s \cdot \mathbf{r}) \cdot [\overleftrightarrow{O}(\mathbf{r}) \cdot \mathbf{E}(\mathbf{r})] \ , \tag{13}$$

where as before $\mathbf{k}_s = k\hat{k}_s$ with $\hat{k}_s = \mathbf{r}_s/|\mathbf{r}_s|$, and we have defined $\hat{e}_s$ such that $\hat{e}_s \cdot \hat{k}_s = 0$ in the far field limit. The form of the scattering amplitude given in Eq. 12 is noninvariant, in the sense that first-order errors made in approximating the field $\mathbf{E}$ in Eq. 13 lead to first-order errors in the approximation for T.

An invariant form for T is obtained by using procedures analogous to those employed by Levine and Schwinger[46] for the scalar case. In particular, a second field, $\tilde{\mathbf{E}}$, and an associated operator, $\overleftrightarrow{\tilde{O}}$, are introduced, Eq. 10 is multiplied by the product $(\overleftrightarrow{\tilde{O}} \cdot \tilde{\mathbf{E}})$, and the result is integrated over the volume of the scatterer to obtain

$$D = N_2 \cdot A \ . \tag{14}$$

Here the integrals N_2 and D are

$$N_2 = \int_{V_0} dV \, (\overleftrightarrow{\tilde{O}} \cdot \tilde{\mathbf{E}}) \cdot [\hat{e}_i \exp(i\mathbf{k}_i \cdot \mathbf{r})] \ , \tag{15}$$

$$D = \int_{V_0} dV \, (\overleftrightarrow{\tilde{O}} \cdot \tilde{\mathbf{E}}) \cdot \mathbf{E} - \int_{V_0} dV \, (\overleftrightarrow{\tilde{O}} \cdot \tilde{\mathbf{E}}) \cdot \int_{V_0} dV' \, \overleftrightarrow{G}_0 \cdot (\overleftrightarrow{O} \cdot \mathbf{E}) \ . \tag{16}$$

Using Eq. 14 to replace $1/A$ in Eq. 12 leads finally to

$$T = N_1 N_2 / 4\pi D \ , \tag{17}$$

the form advertised earlier in Eqs. 2 and 3. Comparison of Eqs. 7 above with Eqs. 13, 15, and 16 shows the similar form, but more complex construction, of the N_1, N_2, and D here.

The requirement that Eq. 17 be stationary with respect to variations about the exact fields $\mathbf{E}$ and $\tilde{\mathbf{E}}$ results in separate integral equations (the Euler equations) for $\mathbf{E}$ and $\tilde{\mathbf{E}}$. (These equations assume that the inverse, $\overleftrightarrow{O}^{-1}$, exists.[23]) The variational requirement suggests the choice $\overleftrightarrow{\tilde{O}} = \overleftrightarrow{O}^{\ddagger}$, where the adjoint $\overleftrightarrow{O}^{\ddagger}$ is defined by $\int dV \, \tilde{\mathbf{E}} \cdot [\overleftrightarrow{O}^{\ddagger} \cdot \mathbf{E}] \equiv \int dV \, [\overleftrightarrow{O} \cdot \tilde{\mathbf{E}}] \cdot \mathbf{E}$. The Euler equation for $\mathbf{E}$ is Eq. 10. The equation for $\tilde{\mathbf{E}}$ is similar to Eq. 10 except that it describes a plane wave of linear polarization $\hat{e}_s$ and amplitude $\tilde{A} = D/N_1$ incident along $-\mathbf{k}_s$ being scattered by an object characterized by $\overleftrightarrow{O}^{\ddagger}$. With these identifications, the field $\tilde{\mathbf{E}}$ is usually called the adjoint field. This reciprocity relationship between $\mathbf{E}$ and $\tilde{\mathbf{E}}$ suggests that a similar relationship should be imposed on the trial approximations for these fields, which are used in performing variational calculations via Eq. 17.

The dyadic Green's function formalism was convenient for deriving the above vector variational expressions[22,23] and for discussing general properties of the variational principle. However, evaluation of the integral D defined in Eq. 16 requires the infinite-space Green's dyadic $\overleftrightarrow{G}_0$ within the source region where the depolarization tensor term, $\overleftrightarrow{L}\delta(\mathbf{r} - \mathbf{r}')$, of Eq. 11 is nonzero. Straightforward evaluation of this depolarization tensor and the corresponding principal value integral proved to be difficult. To remedy this, we used some results from Yaghjian[43] to reexpress D in terms of the scalar Helmholtz Green's function G introduced in Eq. 6 and the text following. The double volume integral in D then becomes[24]

$$\int_{V_0} dV\,(\vec{\tilde{\mathbf{O}}}\cdot\tilde{\mathbf{E}}) \cdot \int_{V_0} dV'\,\vec{\mathbf{G}}_0 \cdot (\vec{\mathbf{O}}\cdot\mathbf{E})$$

$$= \int_{V_0} dV\,(\vec{\tilde{\mathbf{O}}}\cdot\tilde{\mathbf{E}}) \cdot \left[\int_{V_0} dV'\,G\,\frac{1}{k^2}\,\nabla\times\nabla\times(\vec{\mathbf{O}}\cdot\mathbf{E}) - \frac{1}{k^2}\,(\vec{\mathbf{O}}\cdot\mathbf{E}) + \mathbf{S}_{V_0}\right], \quad (18)$$

where $\mathbf{S}_{V_0}$ is a surface integral over the boundary, S_0, of the scatterer involving G and the normal derivative $\partial G/\partial n$. In particular,

$$\mathbf{S}_{V_0} = \int_{S_0} dS'\{(\vec{\mathbf{O}}\cdot\mathbf{E}) \times (\nabla' G \times \vec{\mathbf{I}}/k^2) + [\nabla' \times (\vec{\mathbf{O}}\cdot\mathbf{E})] \times [G\vec{\mathbf{I}}/k^2]\}^{Tr} \cdot \hat{n}' , \quad (19)$$

where superscript *Tr* denotes matrix transpose. Each integral of the right side of Eq. 18 contains integrable singularities of the form $1/R$ and $1/R^{2-\epsilon}$, $\epsilon > 0$. These should, therefore, be simpler to evaluate than the principal value integral and the depolarization tensor required by the nonintegrable $1/R^3$ singularity of $\vec{\mathbf{G}}_0$. Thus, Eq. 18 offers a practical method for evaluating the required variational expression (Eq. 16).

Vector variational expressions were also obtained for perfectly conducting objects.[8,22] The integrals in this case have the form

$$N_1 = \oint_{S_0} \exp(-i\mathbf{k}_s\cdot\mathbf{r})\,(\hat{e}_s\cdot\mathbf{K})\,dS , \quad (20)$$

$$N_2 = \oint_{S_0} (\tilde{\mathbf{K}}\cdot\hat{e}_i)\,\exp(i\mathbf{k}_i\cdot\mathbf{r})\,dS , \quad (21)$$

$$D = \oint_{S_0} dS\,\tilde{\mathbf{K}} \cdot \oint_{S_0} dS'\,\vec{\mathbf{G}}\cdot\mathbf{K}' , \quad (22)$$

where the surface integrals are over the scatterer surface S_0, $\mathbf{K}$ and $\tilde{\mathbf{K}}$ are the original and adjoint surface currents, respectively, and in this case $\vec{\mathbf{G}}$ is the reduced form of Eq. 11 for $\mathbf{r} \neq \mathbf{r}'$. This free-space dyadic Green's function can be shown to be appropriate from the limits taken in Green's theorem at the surface of a perfect conductor. As a result, D in Eq. 22 is evaluated by first performing the $\mathbf{r}'$ integration with $\mathbf{r}$ above S_0 and then letting $\mathbf{r}$ approach S_0 to perform the $\mathbf{r}$ integration.[1,22] For two-dimensional systems, Eqs. 20 through 22 may be reduced to the scalar wave Eqs. 6 above.

STOCHASTIC VARIATIONAL TEST APPLICATIONS

To assess the accuracy and efficacy of the SVP, we have tested it on idealized random models that are complex enough to exhibit cooperative phenomena such as interference and multiple scattering, as well as polarization effects for vector waves. But the test models that are chosen are also simple enough to admit exact solutions, at least for some cases. This is important, since only by knowing exact results can one truly judge the accuracy of approximations. Thus, the models considered are constructed from infinite circular cylinders, which play the role of test model here much like the hydrogen atom in quantum mechanics. We first summarize some results for scalar wave scattering from a classic rough-surface model[47] and then outline both the approach and the results for vector wave scattering from a random dielectric-body model. These examples involve small scatterer-size/wavelength ratios; larger size-parameters are considered in the next section.

Scalar Test Problem

Our first application of the SVP involved calculating the averaged differential cross section, $\langle|T|^2\rangle$, for the scattering of a scalar plane wave by a model rough surface where homogeneous (Dirichlet) boundary conditions are obeyed, i.e., where the wave function vanishes at the surface. The surface consists of a large number, N, of parallel, nonoverlapping hemicylindrical bosses of equal radius randomly distributed on a plane, and the wave is incident normal to the hemicylinders' axes (Fig. 3). The equivalent electromagnetic problem is the scattering of a horizontally polarized wave by an embossed, perfectly conducting plane. We computed the first-order perturbational approximation to $\langle|T|^2\rangle$ and compared it to the stochastic variational improvement of the perturbation approximation.[18,20,21]

In the low-frequency (Rayleigh) limit, both the variational and perturbational approximations were found to be of the form

$$\langle|T|^2\rangle = C(1 - \nu\alpha) , \quad (23)$$

to first order in ν, the "packing density" or area fraction of the plane occupied by the hemicylinders. In both cases the constant C in Eq. 23 is N times the cross section for an isolated hemicylinder. However, the parameter α is equal to 2 for the perturbational approximation and 4.08 for the variational result.

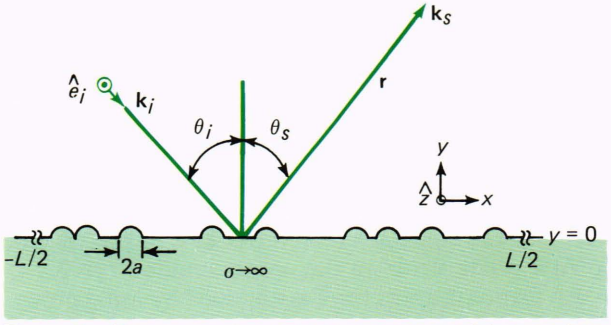

Figure 3—Classic rough-surface scattering model: a stochastic array of the Rayleigh surface elements of Fig. 1b.

In order to investigate the discrepancy beween these two results, we considered a special case of this surface with only two hemicylinders present.[19,20] We obtained the exact solution, as well as the first-order perturbational approximation and its variational improvement. Again we found the result Eq. 23, where now the parameter α equals 1.89 for the exact solution, 2.04 for the variational approximation, and 1 for the perturbational approximation. The variational result is thus the more accurate of the two approximations. A careful examination of these solutions for two hemicylinders revealed that the variational approximation accounts for multiple scattering, but the first-order perturbation approximation, which it clearly improves upon, does not.[19]

Vector Test Case with Inhomogeneous Boundary Conditions

To assess the more general vector SVP, we applied it to a random model of sufficient complexity to exhibit polarization effects, as well as interference and multiple scattering, but again, simple enough to admit an exact solution. Our previous experience led us to consider a random assembly that consists of an ensemble of systems, each of which is a pair of infinitely long, parallel dielectric cylinders of radius a and index of refraction m (Fig. 4). The cylinder separation varies randomly from ensemble member to ensemble member, except that the cylinders are restricted to be nonoverlapping and to have a maximum separation L. (Of course, L must be much smaller than the distance to a field point in order that the asymptotic field and therefore the scattering amplitude is well defined.) The cylinders are illuminated by a plane electromagnetic wave of wavenumber k propagating in the direction $\hat{k}_i$ with linear polarization $\hat{e}_i$, and we examine the component of the scattered field propagating in the direction $\hat{k}_s$ with polarization $\hat{e}_s$.

The scattering configuration in Fig. 4 is the $N = 2$ case of the generic problem of scattering by N randomly separated Rayleigh cylinders. Eventual interest resides in the limit of large N and small packing density, $\nu \equiv N2a/L$. For this reason, the solutions are expressed in powers of packing density, and only linear terms are retained. The $N = 2$ system has the virtue of admitting an exact solution to test the vector stochastic variational results.

The exact field for each cylinder is expressed in standard fashion[19,47,48] as a series of cylindrically outgoing waves centered on the axis of that cylinder. An addition theorem[49] for Bessel functions is then used to translate the waves centered on the axis of one cylinder to a coordinate system centered on the other cylinder. The boundary conditions on the surface of each cylinder can then be easily satisfied and the expansion coefficients in the series determined. This procedure gives a series expansion of the scattering amplitude, and in the small (i.e., Rayleigh) cylinder limit only the leading term contributes.

The variational approximation to the scattering amplitude is obtained by choosing trial functions for the

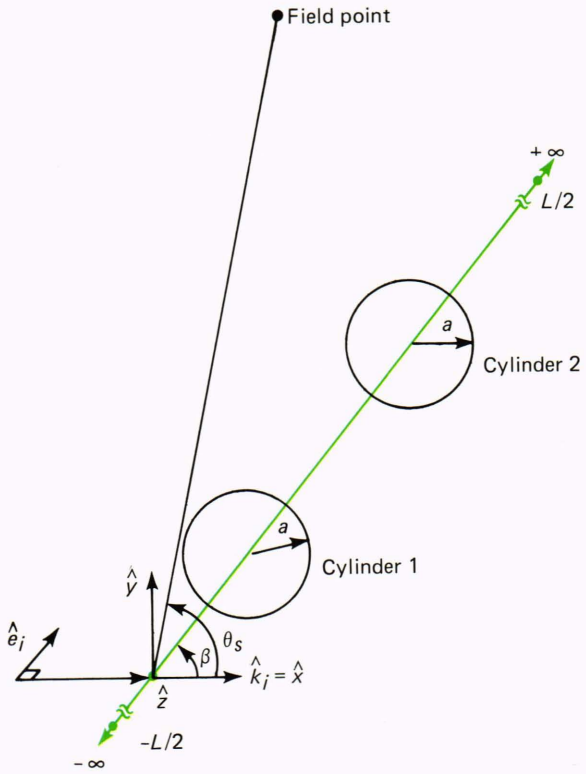

Figure 4—Scattering configuration for two parallel dielectric cylinders with randomly variable separation.

fields $\mathbf{E}$ and $\tilde{\mathbf{E}}$ inside the scatterer. The analysis simplifies in the case of Rayleigh dielectric cylinders, for which $ka \ll 1$ and $mka \ll 1$. Then the fields inside the cylinders for the original and adjoint problems are reasonably approximated by the incoming plane waves, i.e., the Born approximation, $\mathbf{E}(\mathbf{r}) \approx \hat{e}_i \exp(i\mathbf{k}_i \cdot \mathbf{r})$ and $\tilde{\mathbf{E}}(\mathbf{r}) \approx \hat{e}_s \exp(-i\mathbf{k}_s \cdot \mathbf{r})$, is appropriate. We compared[25,26] the exact, Born, and variational solutions to first order in the packing density of the cylinders, $\nu \equiv 4a/L$, for the plane waves incident normal to the axes of the cylinders.

Waves with transverse electric (TE) and transverse magnetic (TM) polarization relative to the cylinders' axes decouple and thus can be analyzed separately. The transverse magnetic wave is relatively simple. To first order in the packing density ν, the exact, Born, and variational solutions for averaged cross section all agree:

$$\sigma \equiv \langle |T_{TM}|^2 \rangle = 2\sigma_0(1 - \nu) , \qquad (24)$$

where σ_0 is the single-cylinder Rayleigh transverse magnetic cross section, and the term proportional to ν is due to interference between the waves scattered by different cylinders. Because the Born result is correct to this order in ν, it follows that multiple scattering affects the transverse magnetic wave only in terms of higher order in ν.

The transverse electric wave is considerably more complicated. The Born approximation has the famil-

iar cosine-squared behavior in scattering angle, θ_s (measured from the forward direction),

$$\sigma^B \equiv \langle |T_{TE}^{(B)}|^2 \rangle = 2\sigma_0 \, (1 - \nu) \cos^2 \theta_s \, . \quad (25)$$

The Born approximation ignores the geometric polarizability of the cylinder in the transverse electric wave.[44] Thus, Eq. 25 disagrees with the single-scattering result,

$$\sigma^S = [2/(m^2 + 1)]^2 \, \sigma^B \, , \quad (26)$$

which is obtained by taking this geometric polarizability into account. A comparison with the exact solution to order ν,

$$\sigma^E = [2/(m^2 + 1)]^2 \, \sigma^B + \sigma_{MS}^E \, , \quad (27)$$

shows that for $m \approx 1$ the multiple scattering effects (through this order in ν) are given by

$$\sigma_{MS}^E = - [2/(m^2 + 1)]^2 \left(\frac{m^2 - 1}{m^2 + 1} \right) \times 2\sigma_0 \, \nu \cos \theta_s \cos (\theta_s - 2\beta) \, , \quad (28)$$

to relative order $(m^2 - 1)/24(m^2 + 1)$, where β is the angle the plane of the cylinder axes makes with the forward direction (Fig. 4). The variational improvement of the Born approximation has the form

$$\sigma^V = [2/(m^2 + 1)]^2 \, \sigma^B + \sigma_{MS}^V \, , \quad (29)$$

where the multiple scattering contribution (last term) is found to be *identical* to the exact contribution (Eq. 28) to the same relative error. The higher order terms of relative size $(m^2 - 1)/24(m^2 + 1)$ in both the exact and variational multiple scattering contributions are discussed and compared in Refs. 25 and 26. The multiple scattering term arises entirely from the surface integral term in Eq. 18.

In summary, comparison of the exact (Eq. 27) and variational (Eq. 29) forms shows that the SVP correctly accounts for the geometric polarizability of the transverse electric wave (even using the Born trial field, which does not); it shows further that, to lowest order in the small parameter $m^2 - 1$, the SVP reproduces the exact multiple scattering contribution.

VARIATIONAL TRIAL-FUNCTION SELECTION

The tests so far described were limited to Rayleigh scatterers, i.e., ones of small size compared to wavelength. For such size-parameters, one generally expects the plane-wave trial fields we adopted to be reasonable first approximations, despite rather gross flaws (e.g., in Eqs. 23 and 25) and even total failures (cf. the Rayleigh transverse magnetic cylinder[30]) when used in *non*invariant formulations. In any event, we have seen that they were susceptible to vast improvement via the SVP. Since our primary concern was to test the SVP solutions against known exact solutions, we gave no initial attention to other size-ranges or other trial functions. But, of course, realistic random scatterers are characterized by ranges of particle dimensions or roughness scales that may include or exceed the wavelengths of interest. Hence, we have devoted considerable subsequent study to the judicious selection or modification of trial functions, and to variational improvement of the Kirchhoff short-wave approximation appropriate to large size-parameters. These studies were mostly restricted to deterministic systems, since the primary interest was in the spectral behavior of the variational integrals (N_1, N_2, and D) that are the same in the deterministic Eqs. 2 and 3 as in the SVP Eq. 5.

Our initial study[27] of trial functions treated a nearly transparent ($m \approx 1$) dielectric sphere, of size-parameter $ka \cdot (m - 1)$, via Eqs. 2 and 7, again with the known exact solution available for comparison. For the simple approximation in which the incident plane wave is used as the trial function, the variational total cross section was found to be accurate to 10 percent up to $ka(m - 1) \approx 0.8$. Modifying the plane wavenumber to that inside the sphere, mk, increased this limit to $ka(m - 1) \approx 1.2$. Introducing an adjustable wavenumber, αk, and determining α variationally, raised the limit to $ka(m - 1) \approx 1.6$. Ultimately, a nonplane (spherical lens) wave function was found the most effective simple trial function tested, raising the limit to $ka(m - 1) \approx 4$ (see Fig. 5). Indeed, reasonably accurate near-forward scatter amplitudes were obtained for $ka(m - 1)$ as large as 10, which for $m = 1.2$ corresponds to a sphere radius of approximately 8λ.

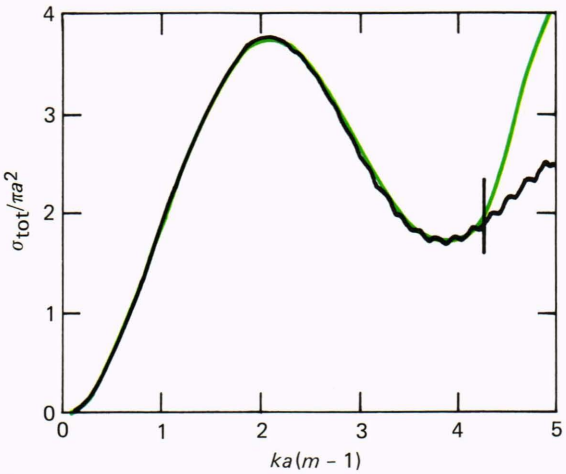

Figure 5—Total scattering cross section (σ_{tot}) for a dielectric sphere of radius a and refraction index $m = 1.2$ as a function of size parameter ($ka(m - 1)$). The variational result using the spherical lens trial function (colored curve) agrees with the exact solution (black curve) within 10 percent up to the vertical bar.

We next investigated the effects of trial function selection on the accuracy achievable with the surface-scattering test model described above (Fig. 3). For plane-wave trial functions, substantially accurate variational amplitudes had been found for $ka \lesssim 1$ and, not surprisingly, complete breakdown at $ka > 1$, where plane waves are a poor starting approximation.[18-21] In order to test the SVP at higher frequencies, we have subsequently investigated the physical optics (Kirchhoff) approximation as a trial function in the variational integrals of Eq. 3. The Kirchhoff trial function is the surface field determined by adopting the tangent-plane approximation for boundary conditions at the scatterer surface and the geometric optics approximation for shadowing. Using this trial function, we found variational improvement not only in the expected regime ($ka > 1$), but also through the important "resonance" region ($ka \sim 1$) and all the way down to the Rayleigh limit ($ka \to 0$). To investigate systematically this all-frequency behavior, we analyzed in detail the classic single-boss model of Rayleigh (Fig. 1b) over all size-parameters, polarizations, and bistatic configurations.[30] This model involves much the same integrals, and *ka* behavior, as the multi-boss random array; but again, its exact solution is available for strict evaluation of results. Sample comparisons of Kirchhoff, variational, and exact calculations are shown in Figs. 1c, 6, and 7 via the curves labeled K, V, and E, respectively. One sees for both transverse magnetic and transverse electric polarization and in both magnitude and phase that the variational (V) curves improve substantially over the Kirchhoff (K) in the latter's domain ($ka \gg 1$), and then nicely follow the exact (E) curves through the transition ($ka \sim 1$) where the Kirchhoff curves have departed significantly from the exact.

The findings over the entire *ka* spectrum from these model calculations[30] are: (a) general variational improvement of the Kirchhoff approximation at high frequencies ($ka \gg 1$); (b) better variational extension into the intermediate-frequency region ($ka \sim 1$) than expected; and (c) substantial low-frequency improvement. Regarding the latter, we find in brief that, whereas Rayleigh limits of the Kirchhoff approximation are totally wrong in wavelength *and* angle dependence (or, by a factor 2 in one case), the variational technique always improves them by correcting the wavelength dependence (and the factor 2). And, while not correcting faulty angular distributions, the variational treatment is found to improve integrated (total) cross sections.

The variational Rayleigh limits are evidently sufficient improvement that they enable the excellent short-wave results to extend satisfactorily through the resonance regime. Nevertheless, the low-frequency accuracy is not uniformly adequate to consider the variational-Kirchhoff approximation a reliable all-frequency method. Furthermore, the Kirchhoff trial function can be awkward for variational calculation, as our forthcoming treatment of variational Kirchhoff divergences for transverse electric polarization will attest. In other words, the canonical Kirchhoff approximation is neither fully adequate nor suitably tractable for variational usage. Instead, it is attractive to exploit the freedom inherent in the variational principle in order to design trial functions that are both simple and effective. For simple scattering models, the liberated approach has yielded extremely accurate all-wavelength variational results.[28,29]

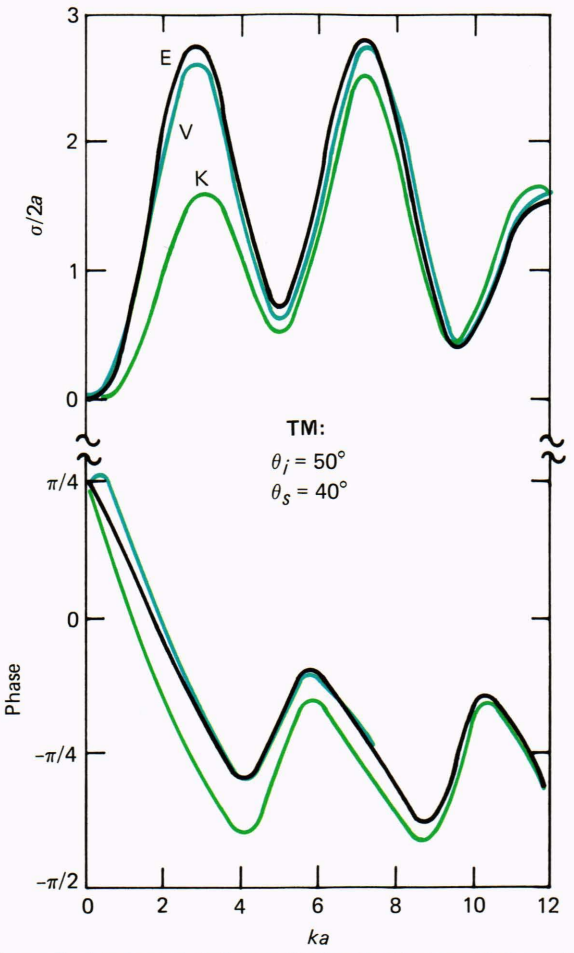

Figure 6—Typical bistatic scattering for the Rayleigh model (Fig. 1b) with horizontal polarization (transverse magnetic, **E** ∥ axis). The scatter cross section relative to boss width ($\sigma/2a$) and phase of scatter amplitude are shown as functions of size-parameter (*ka*) for exact, Kirchhoff, and variational (E,K,V) solutions.

In particular, we have investigated "boundary-Born" approximations, i.e., plane-wave trial functions modified by a parametric function adjustable to suit the boundary conditions. One treats the function or its derivatives (depending on polarization) on the boundary as variational parameters and determines them by the stationarity property of the variational principle. As an example, consider transverse electric plane-wave scattering from the classic Rayleigh model (Fig. 1b). We used a simple modification of the incident plane wave (ψ^{inc}) in which the field near the scattering surface (S_0) is approximated as

$$\psi = \psi^{inc} - \partial\psi^{inc}/\partial n|_{S_0} \cdot f(\rho) \; . \qquad (30)$$

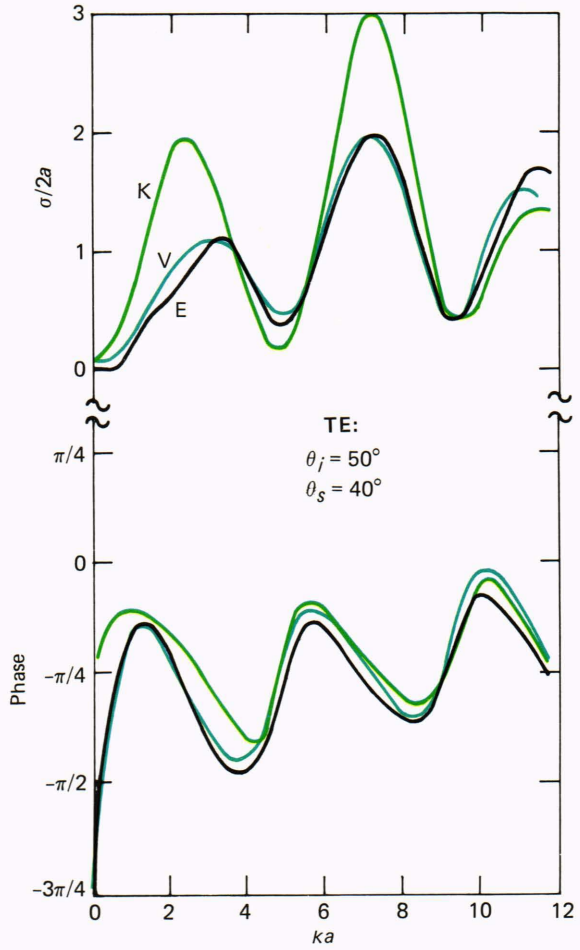

Figure 7—Same as Fig. 6, except with vertical polarization (tranverse electric, **B** ∥ axis).

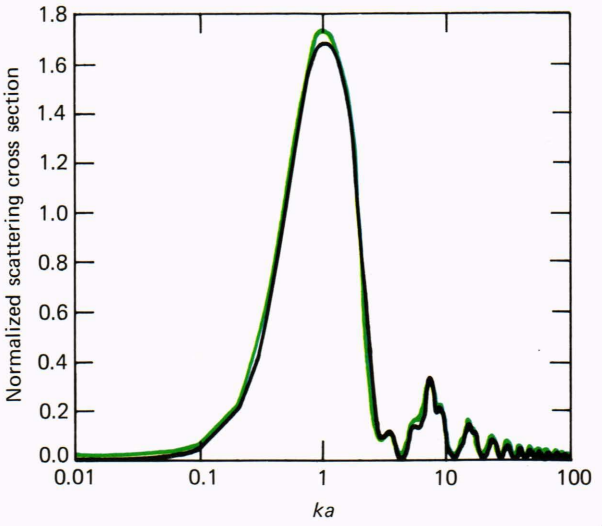

Figure 8—Variational results using the boundary-Born trial function (colored curve) compared to the exact solution (black curve) for the Rayleigh model (Fig. 1b) with vertical polarization (transverse electric) and $\theta_i = 50°$, $\theta_s = -20°$. Note logarithmic size scale (*ka*).

Here ψ represents the magnetic field (**H** ∥ axis), so the boundary condition is $\partial\psi/\partial n = 0$ on S_0. This is identically satisfied by Eq. 30, provided only that $\partial f(\rho)/\partial n|_{S_0} = 1$. We treat $f(\rho)$ on S_0 (i.e., $f(a)$) itself as a variational parameter and determine it by the stationarity condition, $\partial|T|^2/\partial f(a) = 0$.

Figure 8 shows an example of the variational results for (normalized) cross section as a function of size-parameter *ka*. One sees excellent agreement with the exact solution for *ka* ranging over four orders of magnitude around unity. Similarly very accurate broadband results were found for transverse magnetic waves, and also for isolated cylinders with either polarization, by using boundary-Born trial functions analogous to Eq. 30 but appropriate to the pertinent boundary conditions.[28] Thus, choosing simple trial functions that are capable of satisfying the boundary conditions leads to excellent results for perfectly conducting cylindrical scatterers, for radius to wavelength ratios, $ka/2\pi$, ranging from very small to very large.

Presently, trial function design for simple sea-surface radar scattering models is under investigation in collaboration with APL's Space Department. For example, considering a one-dimensional, perfectly conducting corrugated surface, say $z = \zeta(x)$, we again use scalar waves incident normally to the y axis to describe scattering in different polarizations independently. Thus, in horizontal polarization, $\mathbf{E} = \hat{y}E(x,z)$, we approximate the electric field near the surface by the boundary-Born form,

$$E = E^{inc} - E^{inc}\,|_{z=\zeta} \cdot f(x,z)\,, \qquad (31)$$

and the boundary condition $E = 0$ on $z = \zeta(x)$ is guaranteed provided that $f[x,\zeta(x)] \equiv 1$. A simple general form that satisfies this proviso homologously to Eq. 30 is $f(x,z) = g[z - \zeta(x)]$ with $g(0) = 1$. One finds that in the variational integrals (Eq. 2) the parametric function, f, and its derivatives appear only via $\partial f/\partial z|_\zeta$, which for the simple form indicated reduces to $g'(0)$. In that case, there results a completely parameter-independent variational scattering amplitude, which we have evaluated for a sinusoidal surface (again: known exact solution). This variational result has been shown analytically to be in precise agreement with the exact solution in a variety of limiting cases—including both low-frequency and high-frequency limits—even where the trial approximation gives quite wrong noninvariant results. Numerical studies will evaluate the solution for intermediate regimes of scattering parameters. If required, the variational results may be fine-tuned by noting that with a periodic surface, $\zeta(x) = \zeta(x + \Lambda)$, the tuning function, $\partial f/\partial z|_\zeta$, is likewise periodic and representable as a Fourier series, the first term being just the constant $g'(0)$. Of course, if all terms of the series were retained, one expects the exact solution. However, it is important to note that this is not the same as expanding the surface field in a complete set (e.g., Papas' early variational work[3]) because the latter trial function takes no account of the boundary condition. Here it is built into

the trial functions such as Eqs. 30 and 31 from the start.

Another problem presently being investigated is that of a beam with a Gaussian irradiance profile incident on a perfectly conducting, infinitely long cylinder. The case of normal incidence has been analyzed in detail for a boundary-Born Gaussian trial field. The first surprising result was that the adjoint problem is not obtained merely by interchanging $\hat{\mathbf{k}}_i \leftrightarrow -\hat{\mathbf{k}}_s$ in the original Gaussian problem, but rather is the solution of a plane-wave scattering problem with the field incident from $-\hat{\mathbf{k}}_s$ and detected in the direction $-\hat{\mathbf{k}}_i$. Since we know the boundary-Born trial field for a plane-wave scattering problem, this unexpected result does not present a difficulty. Numerical results for transverse magnetic polarization were obtained for a wide variety of system parameters, and the agreement between the exact and variational cross sections was as good as that found earlier in the plane wave problem.

ELECTROMAGNETIC INDUCTION AND VISION

We now leave the subject of variational analysis of wave scattering to summarize some related low-frequency electromagnetic and visual analyses. At low frequencies or high conductivities, such that displacement currents are negligible, pre-Maxwellian methods are commonly adopted (e.g., current-current interaction at a distance). This may seem simpler, but actually can be clumsy, ad hoc, and lead to incomplete solutions; Maxwell field theory instead facilitates precise and complete solution of induction problems.[35-41]

Consider an isotropic linear medium, wherein the electromagnetic Fourier components $\exp[i(\mathbf{k}\cdot\mathbf{r} - \omega t)]$ satisfy the vector wave equation with dispersion relation $k^2 = \epsilon\mu\omega^2 + i\mu\sigma\omega$, where ϵ, μ, σ are permittivity, permeability, conductivity, all assumed scalars here (cf. Eqs. 9). For the optical-to-radar waves considered so far, and outside of good conductors, the wavenumber, k, is nearly real and waves readily propagate. But in the induction regime ($\omega \ll \sigma/\epsilon$),

$$k \approx \sqrt{(i\mu\sigma\omega)} \equiv (1 + i)/\delta\,, \qquad (32)$$

where δ is skin depth, so that $\mathbf{Im}\, k \approx \mathbf{Re}\, k$. This means that "waves" are so strongly damped that they simply diffuse rather than propagate. Thus, instead of incoming plane-waves from infinity being scattered into far-field outgoing waves, here one has to deal with proximate interactions.

For example, in the DISCOS magnetic suspension system, which consists of a metallic cylindrical shell encircling an AC filament, one can treat the levitation as repulsion between the AC current and the eddy currents it induces in the shell. However, a model deduced from current flow at equilibrium gives a misleading physical picture that appears to entail a difficult fabrication problem for the device.[39] The alternative vector field treatment considers the magnetic field of the current filament ($\mathbf{B}_0$) scattering via the shell into an internal field that satisfies the divergenceless vector Helmholtz equation, with k^2 the inductive value (Eq. 32),

$$\nabla \times \nabla \times \mathbf{B} - k^2\mathbf{B} = 0, \quad \text{div}\, \mathbf{B} = 0\,, \qquad (33a)$$

and an external scattered field ($\nabla\psi$) given by Laplace's equation, i.e.,

$$\mathbf{B} = \mathbf{B}_0 + \nabla\psi, \qquad \Delta\psi = 0\,, \qquad (33b)$$

subject only to the boundary condition

$$\mathbf{B} \text{ continuous at interfaces.} \qquad (33c)$$

Equations 33 completely define the field, which then gives the levitational force-torque system by standard formulas, as well as the correct eddy current distribution via $\mathbf{j} = \text{curl}\, \mathbf{B}/\mu$.

The solution of Eqs. 33 was calculated for a great variety of shell constructions and shell-filament orientations for infinitely long, stationary configurations.[39] Subsequently, both finite-length and kinetic-dynamic effects were analyzed. The former[40] yielded good agreement with stationary laboratory measurements. The latter[41] determined the kinetic magnetic torque affecting the spin-orbital dynamics of the suspension over a wide range of parameters and conditions. Along with aiding in malfunction diagnosis and design optimization,[50] it is interesting that already *infinite*-length theory dissolved the apparent need for a difficult fabrication of end-caps for *finite*-length nonhomogeneous shells.[39] This may seem paradoxical but only shows once more the value of exact analysis of idealized models in order to understand practical systems.

For a different example, consider the hydromagnetic field, $\mathbf{b}$, induced by interaction of a given magnetic field, $\mathbf{B}_0$, with a flow field, $\mathbf{u}$, in a weakly conducting fluid. An important instance is oceanic hydromagnetism, where the geomagnetic field interacts with the great variety of seawater motions to induce manifold oceano-magnetic effects.[35] The induced $\mathbf{b}$ is too weak to act back on $\mathbf{u}$ to produce true hydromagnetic radiations (e.g., Alfvén waves) and, as Eq. 32 showed, electromagnetic waves do not propagate. However, an interesting phenomenon that we have called "pseudoradiation" does arise. When the inducing flow $\mathbf{u}$ is a mechanical radiation (e.g., surface or internal gravity waves, or sound), it can carry along with it and thereby propagate the hydromagnetic field. The acoustic case entailing "sonomagnetic" pseudowaves and their scattering by the air-sea interface (see Fig. 9, top) has been analyzed in detail.[36,38]

Sonomagnetic pseudoradiation is described by the inhomogeneous divergenceless vector Helmholtz equation, again with k^2 of Eq. 32,

$$\nabla \times \nabla \times \mathbf{b} - k^2\mathbf{b} = -\mu\sigma\, \text{curl}\, (\mathbf{B}_0 \times \nabla\phi),$$

$$\text{div}\, \mathbf{b} = 0\,. \qquad (34a)$$

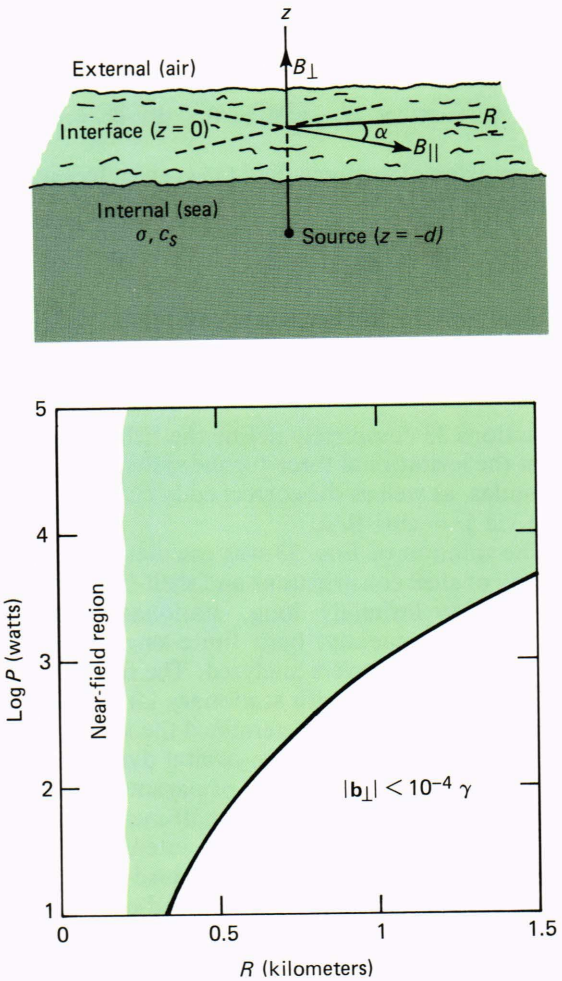

Figure 9—Sonomagnetic pseudowave scattering by the ocean surface (upper sketch) for an undersea acoustic source ($d \ll$ ocean depth) in geomagnetic field of horizontal and vertical components, $B_\parallel$ and $B_\perp$, respectively. The graph shows the source power, P, versus range, R, domain (shaded) in which the sonomagnetic amplitude $|\mathbf{b}_\perp|$ radiated at low altitudes from a 1 hertz vertical acoustic dipole (at any d, see Ref. 36) in a polar ocean exceeds a magnetometer sensitivity of $10^{-4}\gamma$.

Herein the acoustic field is represented by the potential flow, $\mathbf{u} \equiv \nabla\phi$, where ϕ satisfies the scalar Helmholtz equation with acoustic wavenumber k_a,

$$(\nabla^2 + k_a^2)\phi = S(\mathbf{r}), \quad k_a^2 \equiv \omega^2/c_s^2, \quad (34b)$$

in which S is the sound-source distribution and c_s is sound speed. The sonomagnetic field equations (Eqs. 34), subject to the conditions $\mathbf{b}$ continuous and $\phi = 0$ at the air-sea boundary, were solved[36] in quadratures that are analogous to the Sommerfeld integrals of antenna theory but are more complicated in that *two* wavenumbers enter: the electromagnetic k (Eq. 32) and acoustic k_a (Eq. 34b). Analysis showed that the sonomagnetic field, $\mathbf{b}$, not only propagates with the sound but also is transmitted into the (nearly) sound-free air. Therein it is radiated to considerable distances for high-power infrasonic sources, S, as seen in Fig. 9. The time-dependent case (k^2 in Eq. 34a reverting to $-\mu\sigma\partial/\partial t$) was subsequently analyzed for strong pulse sources in an infinite medium, revealing a sonomagnetic shock accompanied by precursor and relaxation waves.[38] Of particular interest are the vector characteristics of the sonomagnetic signal, as opposed to the scalar sound pulse, since they could aid in locating an unknown source.

In closing, it seems felicitous to remark our application of vector-field-analytic methods to a quite different facet of electromagnetic theory: the mathematical description of visual sensation. This has exercised physicists from the founder of electromagnetic theory, Maxwell, through the early vector mathematization (of both space and color) by Helmholtz and Grassman, to the Riemannian geometrization (following Einstein's general relativity) of color theory by Schrödinger. Thus, there is consensus that vision requires a vector theory, despite a period of confusion over just what are the vector components—retinal photon absorptions, or cortical brightness and color sensations.[32] Only recently, however, has the mathematical description evolved to incorporate spatiotemporal variations, thus by definition forming a vector field theory, which we have accordingly analyzed as we did the wave-scattering theory above via a Green's function description.[33]

Maxwell devoted a great deal—by some measures, a third—of his efforts to the analysis of vision. His mature insights that "All vision is color vision. . .," and ". . .essentially a mental science,"[51] seemed lost in subsequent controversies that raged over Helmholtzean "three-color" and Heringean "four- (or more) color" theories. However, controversy dissolved in modern times upon acceptance of the zone concept, viz., that Helmholtz red-green-blue (RGB) color components represent the retinal photoabsorption zone, while Hering's opponent colors (red versus green, blue versus yellow) represent the mental sensation zone. Again to quote Maxwell: ". . . there is one word on which we must fix attention. That word is Sensation."[51] The presently accepted model for visual sensation is shown in Fig. 10.

Recognizing the vector-field character of space-time varying color-brightness vision, $\mathbf{V}(\mathbf{z}')$ as delineated in the Fig. 10 caption, we formulated a general theory in which $\mathbf{V}(\mathbf{z}')$ is a nonlinear vector functional representing all the many physiological operations of the visual system that transmute the quantum absorptions, $\mathbf{Q}(\mathbf{z})$, by cone or rod cells at retinal coordinates $\mathbf{z} \equiv t,x,y$ into the visual sensations.[32] For the large class of vision experiments in which linearization is valid, we expressed the theory by means of an analog to the dyadic Green's function for wave scattering encountered above (cf. Eq. 10), i.e.,[33]

$$\mathbf{V}(\mathbf{z}') = \mathbf{V}_0(\mathbf{z}') + \int d\mathbf{z}\, \vec{\mathbf{F}}(\mathbf{z}',\mathbf{z}) \cdot \Delta\mathbf{Q}(\mathbf{z}) \quad (35)$$

for small-, fast-, or fine-scale fluctuations $\Delta\mathbf{Q} \equiv \mathbf{Q} - \mathbf{Q}_0$ about an ambient state $\mathbf{V}_0,\mathbf{Q}_0$. Notice that we have denoted the Green's dyadic here by $\vec{\mathbf{F}}$, since in

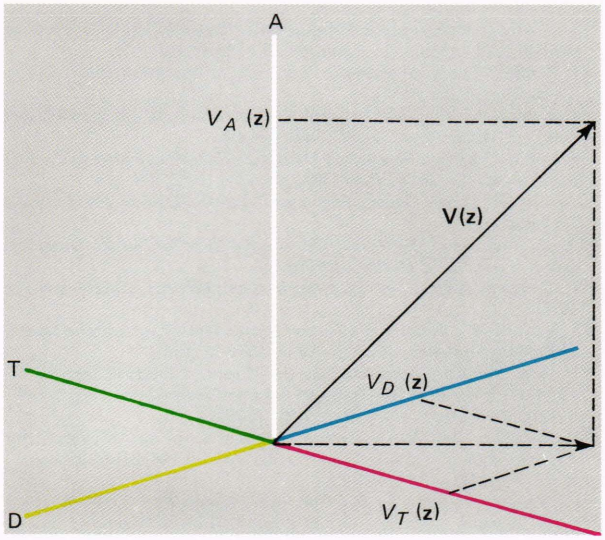

Figure 10—Vector field representation of visual sensation (**V**) in three Cartesian dimensions of achromatic (A), tritanopic (T), and deuteranopic (D) opponent-color sensation. Brightness is measured by $|\mathbf{V}|$, and hue and saturation by ratios V_T/V_D and $V_A/|\mathbf{V}|$, respectively. All are functions of sensory space-time coordinates ($\mathbf{z} \equiv t',x',y'$). (For the color-deficient, including one of the authors: the T axis is red-green, the D is blue-yellow.)

vision the letter *G* is preempted for the color green and unavailable for George Green. The dyadic properties in Eq. 35 refer not to ordinary three-space, however, but to the retinal (RGB) and cortical (ATD, cf. Fig. 10) spaces. This theory has elucidated brightness-contrast studies and standard color models, has provided color vision generalizations of classic space-time brightness laws, has analyzed wavelength-pulse and color-flicker experiments, and has yielded understanding of heterochromatic luminance additivity in flicker and border observations.[32,33]

CONCLUSION

The theoretical researches we have surveyed concern topics that at first can seem too disparate to belong under one title. Yet, the unity of physics relates the different topics closely. One way to appreciate this is to compare the basic field equations (Eqs. 8, 33, and 34). They are all variations on the vector Helmholtz equation that governs general vector field behavior (see Ref. 1, Eq. 13.1.1 and text following). The differences reside in boundary conditions (e.g., Eqs. 1 versus 33b), or in subsidiary conditions (e.g., Eq. 34b), or in the media (e.g., Eqs. 9 versus 32). Vision theory lacks such dynamical field equations (although visual kinematics hints of analogs via the existence of perceptual Lorentz transformations[52]), but its vector field nature (Fig. 10) and Green's function representation (Eq. 35) are well established. Of course the differences in topics lead to dissimilar treatments and consequences. But as emphasized through this review, the mathematical similarities of the different vector field analyses allow them to share common language and lend mutual support.

The core of the research program remains the development of variational techniques for wave scattering calculations, especially for stochastic scatterers. A number of outstanding problems remain to be solved to facilitate application of the technique. For example, formulation of a surface-integral variational principle for penetrable scatterers would ease calculations for lossy dielectric scatterers. Some progress toward this end has been made for high frequencies, and the principle will be tested on a stochastic grating model. Similarly, extension of our variational trial-function design process to the case of imperfect conductors is required. Also, calculations for infinite cylinders need to be extended to finite-length, undulatory, and roughened cylindrical or spheroidal scatterers. Complex macroscopic bodies may then be modeled by combining contributions from a set of such elementary constituent scatterers.

REFERENCES

[1] P. M. Morse and H. Feshbach, *Methods of Theoretical Physics,* McGraw-Hill, New York (1953).

[2] H. Levine and J. Schwinger, "On the Theory of Diffraction by an Aperture in an Infinite Plane Screen, I and II," *Phys. Rev.* **74**, 958-974 (1948) and **75**, 1423-1431 (1949).

[3] C. H. Papas, "Diffraction by a Cylindrical Obstacle," *J. Appl. Phys.* **21**, 318-325 (1950).

[4] H. Levine and J. Schwinger, "On the Theory of Electromagnetic Wave Diffraction by an Aperture in an Infinite Plane Conducting Screen," in *Theory of Electromagnetic Waves—A Symposium,* Wiley Interscience, New York (1951).

[5] C. – T. Tai, "Electromagnetic Back-Scattering from Cylindrical Waves," *J. Appl. Phys.* **23**, 909-916 (1952).

[6] R. D. Kodis, "An Introduction to Variational Methods in Electromagnetic Scattering," *J. Soc. Indust. Appl. Math.* **2**, 89-112 (1954).

[7] R. D. Kodis, "Variational Principles in High-Frequency Scattering," *Proc. Cambridge Philos. Soc.* **54**, 512-529 (1958).

[8] L. Cairo and T. Kahan, *Variational Techniques in Electromagnetism,* Gordon and Breach, New York (1965).

[9] W. S. Ament, "Toward a Theory of Reflection by a Rough Surface," *Proc. IRE* **41**, 142-146 (1953).

[10] C. J. Palermo and L. H. Bauer, "Bistatic Scattering Cross Section of Chaff Dipoles with Application to Communication," *Proc. IEEE* **53**, 1119-1121 (1965).

[11] A. Ishimaru, *Wave Propagation and Scattering in Random Media,* Academic Press, New York (1978).

[12] R. W. Hart and R. A. Farrell, "A Variational Principle for Scattering from Rough Surfaces," *IEEE Trans. Antennas Propag.* **AP-25**, 708-710 (1977).

[13] For a recent review, see E. Lüneburg, "Wave Scattering by Random Surfaces and Application to Natural Surfaces," in *Wave Propagation and Remote Sensing,* Proc. URSI Commission F 1983 Symp., European Space Agency-ESTEC, Noordwijk, The Netherlands, pp. x1iii-1 (1983).

[14] A. K. Fung and M. F. Chen, *Scattering from a Perfectly-Conducting Random Surface—Extinction Method,* Univ. of Kansas, Remote Sensing Laboratory TR 592-3 (Dec 1983).

[15] E. Bahar and D. E. Barrick, "Scattering Cross Sections for Composite Surfaces that Cannot Be Treated as Perturbed Physical Optics Problems," *Radio Sci.* **18**, 129-137 (1983).

[16] E. Bahar, C. L. Rufenach, D. E. Barrick, and M. A. Fitzwater, "Scattering Cross Section Modulation for Arbitrarily Oriented Composite Rough Surfaces: Full Wave Approach," *Radio Sci.* **18**, 675-690 (1983).

[17] E. Bahar and M. A. Fitzwater, "Scattering Cross Sections for Composite Rough Surfaces Using the Unified Full Wave Approach," *IEEE Trans. Antennas Propag.* **AP-32**, 730-734 (1984).

[18] E. P. Gray, R. W. Hart, and R. A. Farrell, "A New Variational Approach to Scattering by Random Media or Rough Surfaces," in *Proc. Open Symposium,* URSI Commission F, pp. 111-115 (1977).

[19] J. A. Krill and R. A. Farrell, "Comparisons Between Variational, Perturbational, and Exact Solutions for Scattering from a Random Rough Surface Model," *J. Opt. Soc. Am.* **68**, 768-774 (1978).

[20] E. P. Gray, R. W. Hart, and R. A. Farrell, "An Application of a Variational Principle for Scattering by Random Rough Surfaces," *Radio Sci.* **13**, 333-343 (1978).

[21] E. P. Gray, R. W. Hart, and R. A. Farrell, *A Variational Approximation for the Scattering of Scalar Waves by Stochastic Surfaces,* JHU/APL TG 1322 (1979).

[22] J. A. Krill and R. H. Andreo, "Vector Stochastic Variational Principles for Electromagnetic Wave Scattering," *IEEE Trans. Antennas Propag.* **AP-28**, 770-776 (1980).
[23] R. H. Andreo and J. A. Krill, "Vector Stochastic Variational Expressions for Scatterers with Dielectric, Conductive, and Magnetic Properties," *J. Opt. Soc. Am.* **71**, 978-982 (1981).
[24] J. A. Krill, R. H. Andreo, and R. A. Farrell, "A Computational Alternative for Variational Expressions that Involve Dyadic Green Functions," *IEEE Trans. Antennas Propag.* **AP-30**, 1003-1005 (1982).
[25] J. A. Krill, R. H. Andreo, and R. A. Farrell, "Variational Calculations of Electromagnetic Scattering from Two Randomly Separated Rayleigh Dielectric Cylinders," *J. Opt. Soc. Am.* **73**, 408-410 (1983).
[26] J. A. Krill, R. H. Andreo, and R. A. Farrell, *Calculation Procedures for Variational, Born, and Exact Solutions for Electromagnetic Scattering from Two Randomly Separated Dielectric Rayleigh Cylinders,* JHU/APL TG 1344 (1983).
[27] M. R. Feinstein and R. A. Farrell, "Trial Functions in Variational Approximations to Long Wavelength Scattering," *J. Opt. Soc. Am.* **72**, 223-231 (1982).
[28] J. A. Krill, J. F. Bird, and R. A. Farrell, "Trial Functions in Variational Calculations," in *Proc. 1982 CSL Scientific Conf. on Obscuration and Aerosol Research,* R. H. Kohl & Assoc., pp. 201-209, (1983).
[29] J. A. Krill and R. A. Farrell, "The Development and Testing of a Stochastic Variational Principle for Electromagnetic Scattering," in *Wave Propagation and Remote Sensing,* Proc. URSI Commission F 1983 Symp., European Space Agency-ESTEC, Noordwijk, The Netherlands, pp. 299-307 (1983).
[30] J. F. Bird, "Analysis of All-Frequency Variational Behavior of the Kirchhoff Approximation for a Classic Surface-Scattering Model," *J. Opt. Soc. Am. A* **2**, 945-953 (1985).
[31] R. A. Farrell, C. B. Bargeron, W. R. Green, and R. L. McCally, "Collaborative Biomedical Research on Corneal Structure," *Johns Hopkins APL Tech. Dig.* **4**, 65-79 (1983).
[32] R. W. Massof and J. F. Bird, "A General Zone Theory of Color and Brightness Vision I. Basic Formulation," *J. Opt. Soc. Am.* **68**, 1465-1471 (1978).
[33] J. F. Bird and R. W. Massof, "A General Zone Theory of Color and Brightness Vision II. The Space-Time Field," *J. Opt. Soc. Am.* **68**, 1471-1481 (1978).
[34] J. F. Bird, R. W. Flower, and G. H. Mowbray, "Analysis of the Retina via High Frequency Electroretinography," *Biophys. J.* **29**, 379-396 (1980).
[35] J. F. Bird and H. Ko, *Ocean Magnetics I. Fundamental Survey and Estimates of Induction Phenomena,* JHU/APL TG 1315A (1977).
[36] J. F. Bird, "Hydromagnetism Induced by Submerged Acoustic Sources: Sonomagnetic Pseudoradiation," *J. Acoust. Soc. Am.* **62**, 1291-1296 (1977).
[37] J. F. Bird, "Hydromagnetic Perturbations Due to Localized Flows: An Eddy Theorem," *Phys. Fluids* **22**, 585-586 (1979).
[38] J. F. Bird, "Sonomagnetic Pulses from Underwater Explosions and Implosions," *J. Acoust. Soc. Am.* **67**, 491-495 (1980).
[39] J. F. Bird, "Theory of Magnetic Levitation for Biaxial Systems," *J. Appl. Phys.* **52**, 578-588 (1981).
[40] J. F. Bird, "Levitational End-Effects in a Cylindrical Magnetic Suspension," *J. Appl. Phys.* **52**, 6032-6040 (1981).
[41] J. F. Bird, "Kinetic Torque and Dynamic Behavior in a Magnetic Levitation Device," *J. Appl. Phys.* **53**, 1326-1333 (1982).
[42] C. – T. Tai, *Dyadic Green's Functions in Electromagnetic Theory,* Intext, Scranton (1971).
[43] A. D. Yaghjian, "Electric Dyadic Green's Functions in the Source Region," *Proc. IEEE* **68**, 248-263 (1980).
[44] H. C. van de Hulst, *Light Scattering by Small Particles,* Dover, New York (1981).
[45] J. Van Bladel, "Some Remarks on Green's Dyadic for Infinite Space," *IRE Trans. Antennas Propag.* **AP-9**, 563-566 (1961).
[46] H. Levine and J. Schwinger, "On the Theory of Electromagnetic Wave Diffraction by an Aperture in an Infinite Plane Conducting Screen," *Comm. Pure Appl. Math.* **3**, 355-391 (1950).
[47] V. Twersky, "Multiple Scattering of Radiation by an Arbitrary Planar Configuration of Parallel Cylinders and by Two Parallel Cylinders," *J. Appl. Phys.* **23**, 407-414 (1952).
[48] G. Olaofe, "Scattering by Two Cylinders," *Radio Sci.* **5**, 1351-1360 (1970).
[49] G. N. Watson, *A Treatise on the Theory of Bessel Functions,* 2nd ed., Cambridge University Press, New York (1966).
[50] V. L. Pisacane et al., *TIP-III DISCOS Study Group Report,* JHU/APL SDO-5592 (1980).
[51] J. C. Maxwell, "On Colour Vision," *Scientific Papers,* Vol. II, 267-279, Dover reprint (1890).
[52] T. Caelli, W. Hoffman, and H. Lindman, "Subjective Lorentz Transformations and the Perception of Motion," *J. Opt. Soc. Am.* **68**, 402-411 (1978).

ACKNOWLEDGMENT—This work has been supported in part by the Army, the Navy, the Strategic Defense Initiative Office, the National Aeronautics and Space Administration, and the National Institutes of Health. We are pleased to acknowledge a number of members of the Laboratory's staff who made important contributions to the analyses that are reviewed in this article. They include: Robert W. Hart, Assistant Director for Research and Exploratory Development; Jerry A. Krill and Matthew R. Feinstein, presently in the Fleet Systems Department; David E. Freund of the Research Center; Ernest P. Gray of the Space Department and members of the DISCOS Study Group in that Department; Harvey W. Ko of the Submarine Technology Department; and Robert H. Andreo, who is no longer at APL. It is also a pleasure to acknowledge collaboration on the color vision theory with Robert W. Massof of the Wilmer Institute of The Johns Hopkins University School of Medicine.

THE AUTHORS

JOSEPH F. BIRD (left) is a physicist in the Theoretical Problems Group. He joined the Milton S. Eisenhower Research Center in 1958 and was appointed to the Principal Professional Staff in 1962. He was born in Scranton, Pa., in 1930 and earned an A.B. degree in physics from the University of Scranton in 1951 and a Ph.D. degree in theoretical physics from Cornell University in 1958. Dr. Bird's research results at APL have been published as journal articles in various fields: combustion instability in solid-fuel rockets, star formation theory and cosmogony, psychophysics and electrophysiology of vision, oceano-hydromagnetics theory, neural noise modeling, the theory of chromatic visual sensations, electromagnetic levitation calculations, and wave scattering theory. The variety of these researches largely reflects the diversity of his collaborations with other APL departments and the Johns Hopkins Medical School.

RICHARD A. FARRELL (right) is a physicist and the supervisor of the Theoretical Problems Group in the Milton S. Eisenhower Research Center. Born in Providence, R.I., he obtained a B.S. degree from Providence College in 1960, an M.S. from the University of Massachusetts in 1962, and a Ph.D. from The Catholic University of America in 1965. Dr. Farrell's research interests include relating the cornea's structure to its function, especially relative to its light-scattering properties; developing theoretical methods for calculating wave scattering in random media; and analytic treatments of the statistical mechanics of phase transitions. APL's collaborative efforts with the Johns Hopkins Medical School stimulated his interest in biomedical problems when he joined APL in 1965. The scattering techniques used in his corneal research and the Laboratory's interest in alterations of the sea surface led to his involvement in fundamental investigations of scattering by random systems. Dr. Farrell is the principal investigator on contracts and grants from the Army and the National Eye Institute and is an investigator on the Laboratory's Space Sciences Consortium in support of the Strategic Defense Initiative. He is a member of various professional organizations, including the American Physical Society, the Optical Society of America, the Association for Research in Vision and Ophthalmology, the International Society for Eye Research, and the New York Academy of Sciences.